Scanning tunneling microscopy head having integrated capacitive sensors for calibration of scanner displacements

G. B. Picotto, S. Desogus, Š. Lányi, R. Nerino, and A. Sosso

Citation: Journal of Vacuum Science & Technology B **14**, 897 (1996); doi: 10.1116/1.589170
View online: http://dx.doi.org/10.1116/1.589170
View Table of Contents: http://scitation.aip.org/content/avs/journal/jvstb/14/2?ver=pdfcov
Published by the AVS: Science & Technology of Materials, Interfaces, and Processing

Scanning tunneling microscopy head having integrated capacitive sensors for calibration of scanner displacements

G. B. Picotto and S. Desogus
CNR-Istituto di Metrologia "G. Colonnetti," Strada delle Cacce 73, 10135 Torino, Italy

Š. Lányi
Institute of Physics, Slovak Academy of Sciences, Dubravska cesta 9, 84228 Bratislava, Slovakia

R. Nerino and A. Sosso
Istituto Elettrotecnico Nazionale "G. Ferraris," Strada delle Cacce 91, 10135 Torino, Italy

(Received 24 July 1995; accepted 23 November 1995)

Scanning tunneling microscopy heads having some tip–displacement measurement capability are essential for quantitative and accurate measurements. A scanning tunneling microscopy head based on a bimorph parallelogram scanner with a metallized glass cube situated above the tunneling tip is described. The cube acts as a counterelectrode or as a mirror for capacitance-based and interferometric measurements of scanner displacements. The capacitive sensors are mounted on differential screws facing the cube in such a way that the lateral Abbe error in the measurement of actual tip–displacements is minimized. The sensor electronics uses a Howland-type alternating current source, and has a deviation from linearity of less than 0.15% up to 30 μm and a low frequency bandwidth of 1 kHz.

I. INTRODUCTION

The micropositioning mechanisms of scanning probe microscopes (SPM) are usually based on piezoceramic elements that suffer from nonlinearity, hysteresis, creep, dependence on humidity, scanning speed, etc. All these effects cause specific distortions of images and complicate the use of such techniques in the more precise applications. Usually, the only way of suppressing these drawbacks is calibration using suitable test structures and the introduction of some sort of corrections. Distortions are usually severe for large fields of view. In some applications, such deficiencies are not tolerable. This is the case of dimensional metrology in the micrometer and nanometer scale. Recently, attempts were made to solve the problem by combining the scanner with an independent measuring tool represented by capacitive sensors[1–4] or by on-line use of an interferometer.[5] The idea was to collect data on the true position of the probe or to use close-loop control of its displacements.[6]

The scanning tunneling microscopy (STM) head we presented in Ref. 2 used a flexible parallelogram made of piezoceramic bimorphs deforming to a double S shape.[7,8] This shape has the advantage of scanning in a plane, a property that cannot be simply achieved with the more popular and simple tubes. The parallelogram also has well-defined positions, namely, in the corners and at the centers of the oblong bimorph plates, where the movement is purely translational, i.e., free of rotation, at least as a first approximation, provided the material of the elements is perfectly homogeneous. These positions are ideally suited for mounting the electrodes of the capacitive sensors or the mirrors for interferometric measurements. A similar approach has been followed in Ref. 3.

The capacitance of a parallel plate capacitor depends on the overlapping area of its plates and on their separation. Of course, changing the separation will result in additional capacitance variations if the plates are not parallel, or their relative movement is not strictly translational. If one plate is fixed and the other is coupled to a moving element whose position has to be monitored, such as a tube-shaped SPM scanner, capacitance variations can be quite successfully used for position monitoring on a more or less empirical basis.[1,9] However, the real advantage of a well-defined capacitive sensor is the possibility to calculate the capacitance as a function of position to very high accuracy.[10]

The capacitive sensors in Ref. 2 used fixed active electrodes and very light mobile counterelectrodes that could be alternatively used for interferometric verification of the calculated capacitance versus displacement dependence. The circular active electrodes are surrounded by a guard ring in order to reduce the fringe effects. In contrast to position monitoring by capacitance measurements, interferometric measurements suffer from the unwanted rotations of the moving mirror that may cause loss of interferometric beat. Depending on the distance between the reference and moving mirrors and the interferometric setup, rotations exceeding 1 mrad may be critical. Furthermore, the rotations of the scanner may cause a significant Abbe error, when the distance between the tip and the position monitor is large. With the head described in Ref. 2, the STM tip is situated at the center of the parallelogram, while the pair of sensors for y displacements are in the corners, thus giving rise to a significant Abbe offset. Also, the change of the distance between the neighboring corners, caused by the bending of the plate connecting them result in small errors. Although these may be minimized by taking the difference of the readings from pairs of sensors, in practice this may be a disadvantage.

The inverse dependence of the capacitance on plate dis-

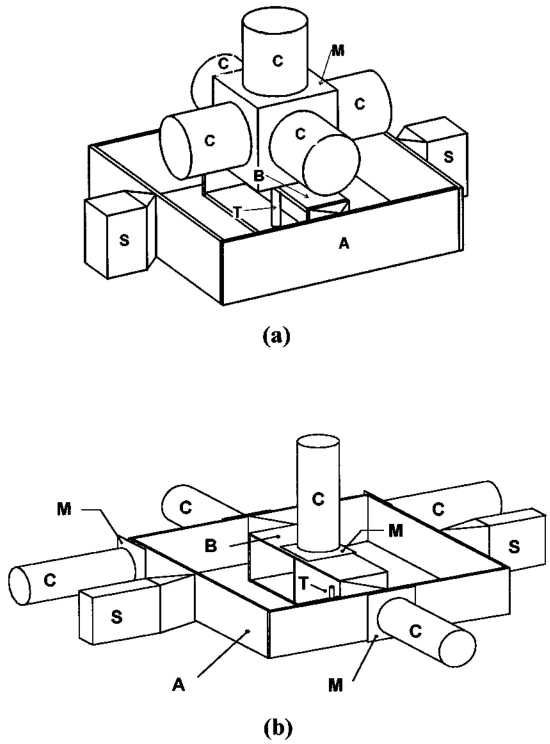

FIG. 1. Schematic drawing of the new head (a) and the old head (b). S—support, A—*xy* frame, B—*z*-deflection plates, C—capacitive sensors, M—cube counterelectrodes, T—tip holder.

tance is an inconvenient property. At a given voltage noise of the capacitance meter, such dependence results in an uncertainty proportional to distance (relative error constant). It is therefore better to use the capacitor as a reactance sensor, which may then form a linear displacement to voltage transducer.[2,11]

II. DESIGN OF THE HEAD

The flexible parallelogram (Fig. 1) made up of 30 mm$\times$6 mm$\times$1 mm bimorph plates forming a square ensures scanning in the *xy* plane. Two bimorphs of 25 mm$\times$6 mm$\times$0.8 mm form a parallel arrangement for movement along the *z* axis. V-shaped spacers made of resin (Araldite) are used to connect the *z* plates to the central part of two opposite plates of the square, which itself is fixed to the support in the center of the other two plates of the square. The bimorphs are polarized by sections in opposite directions, and the internal electrode is the active one, while the outer ones form a shield and are grounded.[8] The tip holder consists of a 0.3 mm steel capillary glued into a hole drilled at the center of the two *z* plates. The head was designed to be used with a homemade STM device.[12]

Compared to the head described in Ref. 2, the new scanner uses smaller plates and has a higher mechanical rigidity, although it covers a smaller range. In the present design, the five metallized mirrors used as counterelectrodes of the capacitive sensors along the three axes of the scanner have been replaced by a metallized cube above the tunneling tip (Fig. 1). The lateral Abbe offset in the *xy* plane between the tip and transducers is minimized, at the cost of a larger vertical offset. The tip and the cube are now both mounted on the same *z*-deflecting structure and, therefore, the effects due to imperfect stage symmetry resulting from the bimorph material and assembling are minimized.

With the transducers using separate mirrors/counters electrodes,[2] the capacitive sensor was connected into the feedback of an operational amplifier, i.e., the active electrode was connected to the inverting input and the counterelectrode to the output.[2] Such an approach is very simple but less advantageous in the case of the cube/counterelectrode, because it would require independent shielded leads to each isolated face of the cube. Therefore, in the new solution, a constant amplitude ac current is fed to the active electrode of each sensor and the counterelectrodes are grounded. Thus, all the metallized faces of the cube remain interconnected and only one common ground connection is required. Such a connection is available through the grounded outer electrodes of the bimorphs and no additional leads to the cube are needed. The cube was made from a hollow Zerodur block to make it lighter and with shape details to accommodate it on the *z* plate. The faces of the cube were polished to $\lambda/4$ flatness and metallized with Cr and Au layers. The right angle accuracy of the cube is within 0.1 mrad.[13]

The parallelogram scanner is fixed to the support in such a way as to optimize the alignment between the five sensors and the cube. Homemade differential screws are used for approach and fine positioning of the sensors to the metallized cube. The differential screws are fixed to the support into precise cylindrical seats facing the cube. The frame support is made of low thermal-expansion steel.

Two different types of capacitive sensors, one of metallized fused silica and the other of low thermal-expansion steel, have been tested. Both sensors have polished faces with the active electrode surrounded by a larger guard ring. The capacitance is inversely proportional to the distance between electrodes (i.e., $1/C$ versus distance d is linear) only if a uniform field approximation is used. In other words, the model does not take account the finite area of real sensors, which produces a field slightly spreading from the smaller active electrode to the larger counterelectrode (fringe effect). With very small distances, the equivalent area approaches that of the smaller electrode. To limit the spreading at larger distances, the active electrode is surrounded by a large planar guard ring, held at the same potential as the active electrode. With this ring, spreading is limited by half of the gap between the active electrode and the guard.[14] Therefore, the gap must be very narrow. The metallized fused silica sensor has a narrower gap than the steel sensor; on the other hand, fringe effect reduction is incomplete with the former type, since a thin strip connection to the active electrode interrupts the guard.

III. CAPACITANCE MEASUREMENT ELECTRONICS

The capacitive sensors to yield a linear output signal versus displacements require a measurement technique substantially differing from those commonly used. The linearity is achieved by measuring the voltage across the sensor fed by a constant amplitude ac current. Although standard methods may yield a lower uncertainty of the capacitance value, such measurement offers several advantages in this case, since the displacement should be known in real time and precision requirements are not extremely high. The fast availability of data is interesting both in z-axis measurement and along the x and y axes, where working in a control loop is foreseen.

There are few ways of supplying a constant ac current into a grounded load. Some complications result from the fact that the load is a capacitor. To prevent the current from being affected by possible frequency instability, it is advantageous to use a capacitor also as a reference element. This complicates the dc paths, which must affect neither current sensing nor drain any significant fraction of the output current. We have chosen a Howland-type circuit,[15] with which the effect of all parasitic capacitances can easily be eliminated except the common mode input capacitance of the sensing operational amplifier. This capacitance is connected in parallel to the sensor; thus, it would drain away a part of the output current, causing deviations from linearity of $1/C$ versus displacements.

The acceptable amount of parasitic capacitance depends also on the working range. Our sensors were designed for a maximum capacitance change between 1 and 100 pF over a 200 μm range. The minimum capacitance over a smaller range in the z direction (<15 μm) would be above 10 pF. As the actual requirement for the x and y axes is 5 to 30 pF, the requirements on capacitance suppression are also less stringent. Nevertheless, the acceptable parasitic capacitance is at most a few femtoFarad.

The effect of the common mode input capacitance can be minimized by keeping the ac voltage across it as small as possible. This has been achieved by careful shielding and bootstrapping the buffer stage and the guard ring of the sensor. The extent to which this may be successful depends on the available open loop gain of the amplifier at the operating frequency. For slow scanning in the y or x directions, relatively small low frequency bandwidths of a few Hertz and tens of Hertz, respectively, may be satisfactory. Therefore, the working frequency may also be moderate, e.g., 10 kHz. As the response in the z direction must be significantly faster, a higher operating frequency is inevitable in order to allow for good filtering after demodulation and to achieve an acceptable bandwidth of approximately 1 kHz. The choice is a tradeoff between bandwidth, on the one hand, and suppression of the parasitic capacitances and good smoothing on the other. We have tested the electronics at 50 kHz. The simplified circuit diagram of the current generator is seen in Fig. 2.

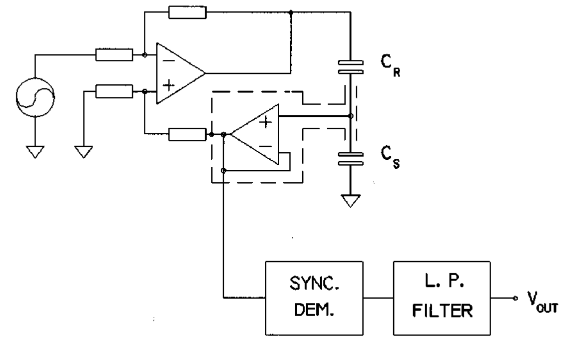

FIG. 2. Schematic circuit of transducer electronics. Cr—reference capacitor, Cs—capacitive sensor.

IV. EXPERIMENT AND RESULTS

By driving the bimorph plates at voltages of ±150 V, the scanner sampling area resulted in about 30 μm$\times$30 μm, with a z range of about 15 μm. The lowest resonance frequencies of the scanner were about 0.85, 0.8, and 1.5 kHz for the x, y, and z axes, respectively. The resonance frequencies were estimated from the output voltage versus frequency as measured from one axis of the frame, while another axis was driven with a sine wave generator at 15 V. The cube was made as light as possible to avoid increasing seriously the mass of the scanner. The x, y, and z resonance frequencies without the cube were 1.1, 1, and 2 kHz, respectively. Mutual coupling between the axes was first estimated in the same way as the resonance frequencies and, subsequently, by means of interferometric measurement of cube displacements along one axis, when another axis was driven in steps to ±150 V. Coupling was about 1% between the x and y axes and 0.3% between both the x and z, and the y and z axes. Pitch, roll, and yaw rotations of the scanner were measured by means of an autocollimator facing the cube and by driving the scanner along the border of its working volume. Rotations within ±25, ±20, and ±10 μrad were observed around the xy, yz, and xz planes, respectively. These rotations are at present the main error source in the measurement of the actual tip displacements. Because of the vertical Abbe offset between the tip and the sensors, errors as large as ±200 nm may occur when scanning over the full working volume of the scanner.

The stand-alone calibration of the current source using precise capacitors showed deviations of the current below ±0.05% over the output range. The capacitive sensors were calibrated individually on the head by means of a differential interferometer (HP 10719A) in a single-pass configuration. By driving the scanner along one axis, displacements were measured at one side of the cube by one capacitive sensor, while the face of the cube on the opposite side of the sensors was used as the moving mirror of the interferometer. The displacements were sampled at steps of integer λ to minimize the nonlinearity of the interferometer. Deviation from linearity of the capacitance-based measurements was well within 0.15% (Fig. 3) even with a large scan of 30 μm. A repeatability within 0.1% of the sensitivity of the capacitive transducers was obtained from a number of full-scan measurements taken at different distances between the sensors and the cube face. Because of both fringe effects and misalignment between the electrodes, deviation from linearity was higher when the sensor approached the cube up to distances lower than half the gap between the active electrode

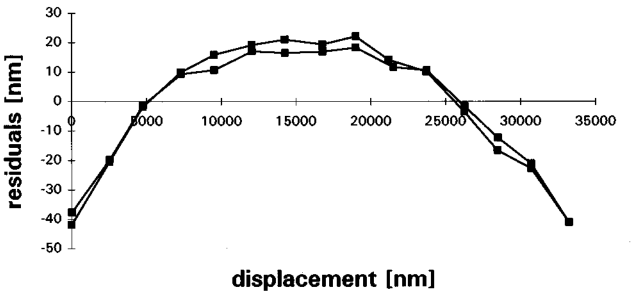

FIG. 3. Residuals of a linear fit of displacements measured by interferometer and sensor for a full scan loop along the x axis.

and the guard. Misalignment between the electrodes, which results from assembling as well as from pitch, roll, and yaw errors of the differential screws used for positioning the sensors in front of the cube, was estimated to be within 1 mrad. This estimate was confirmed by the minimum output voltage obtainable from the transducers, before the active electrode touched the cube.

To test the dynamic performance of the measuring system, a square-wave voltage was applied to the x axis of the scanner and the resulting displacement of the cube was monitored with the interferometer and the sensor at the opposite sides of the cube. Figure 4 shows the oscilloscope traces of the two signals from a step of about 20 nm. The interferometer output was taken from a phase meter (HP 3575A) having a relatively high settling time at the frequency of the heterodyne interferometer. The transducer output was displayed using a preamplifier with gain of 10. In the present setup, the bandwidth of the capacitive transducer is about 1 kHz. Its output showed a transient oscillation near 850 Hz, which corresponds to the observed x-axis resonance frequency of the scanner, whereas the slow output of the phase meter revealed a small oscillation with a frequency of about 50 Hz, probably due to residuals vibrations of the support table. The rms noise of the transducers is below 0.5 nm, with the output voltage range optimized for the 30 μm range, with a 1 kHz bandwidth. Further noise reduction is expected in the x and y directions after reduction of the electronics bandwidth, as well as by optimizing the transducer output voltage for the 15 μm range of the z axis.

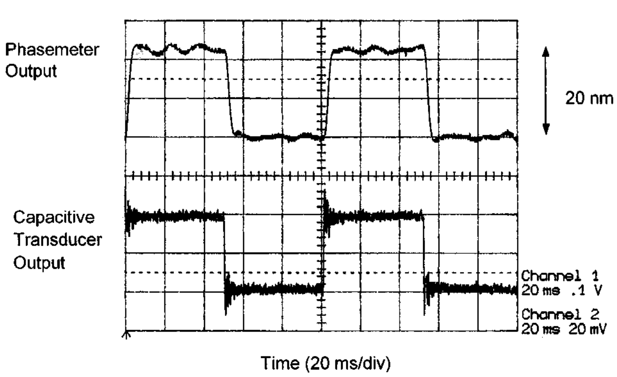

FIG. 4. Response of phasemeter and transducer to a square-wave excitation of the scanner.

V. CONCLUSIONS

A STM head using a flexible parallelogram scanner made of bimorph plates and a metallized Zerodur cube mounted above the tunneling tip, with integrated capacitive sensors for measurement of the scanner displacements, has been constructed. In the present design, the lateral Abbe offset between the sensors and the tip has been minimized. The head offers a range of 30 μm$\times$30 μm$\times$15 μm with minimum resonant frequencies of 0.85, 0.8, and 1.5 kHz along the x, y, and z directions, respectively. Pitch, roll, and yaw errors are still present at scanning. Further attempts to optimize the assembling are in progress.

The capacitive transducers use a new electronics based on a Howland-type ac constant amplitude current source. The electronics shows an accuracy better than 0.05% when tested with precision capacitors. The whole assembly of the transducers show a deviation from linearity within 0.15%. A bandwidth of 1 kHz with a resolution of 0.5 nm has been achieved with the sensor optimized for a 30 μm range.

ACKNOWLEDGMENT

The authors wish to thank Franco Mauro of IMGC for all the precision machining needed in the present work.

[1] J. E. Griffith and D. A. Grigg, J. Appl. Phys. **74**, R83 (1993).
[2] S. Desogus, Š. Lányi, R. Nerino, and G. B. Picotto, J. Vac. Sci. Technol. B **12**, 1665 (1994).
[3] O. Jusko, X. Zhao, and G. Wilkening, *Proceedings of the 8th International Precision Engineering Seminar* (Elsevier, New York, 1995), p. 187.
[4] O. Jusko, X. Zhao, H. Wolff, and G. Wilkening, Rev. Sci. Instrum. **65**, 2514 (1994).
[5] J. Schneir, T. H. McWaid, J. Alexander, and B. P. Wilfley, J. Vac. Sci. Technol. B **12**, 3561 (1994).
[6] E. C. Teague, J. Vac. Sci. Technol. B **7**, 1898 (1989).
[7] P. Muralt, D. W. Pohl, and W. Denk, IBM J. Res. Dev. **30**, 443 (1986).
[8] Š. Lányi and M. Ozvold, Ultramicrosc. **42–44**, 1664 (1992).
[9] J. E. Griffith, G. L. Miller, C. A. Green, D. A. Grigg, and P. E. Russell, J. Vac. Sci. Technol. B **8**, 2023 (1990).
[10] W. C. Heerens, J. Phys. E **19**, 897 (1986).
[11] G. L. Miller, R. A. Boie, P. L. Cowan, J. A. Golovchenko, R. V. Kerr, and D. A. H. Robinson, Rev. Sci. Instrum. **50**, 1062 (1979).
[12] G. B. Picotto, S. Desogus, and G. Barbato, Rev. Sci. Instrum. **64**, 2699 (1993).
[13] SILO snc, Via D. Burchiello 4r, 50124 Firenze, Italy.
[14] S. Desogus, Š. Lányi, R. Nerino, G. B. Picotto, and A. Sosso, Proc. XIII IMEKO World Congress **3**, 1690 (1994).
[15] J. Steele and T. Green, Electron. Des. 61 (1992).